A Study on Preparation of Failure Parameters for Ductile Polymers

Kunio Takekoshi and Kazukuni Niwa

TERRABYTE Co., Ltd, NOV BLDG 3F, 3-10-7, Yushima, Bunkyo-ku, Tokyo, 113-0034, Japan

Abstract

A study on preparation method of failure parameters for ductile polymers is presented using experimental results of high-speed tensile test for polycarbonate and simulation results based on Semi-Analytical Model for Polymers (SAMP) constitutive model [1] in LS-DYNA®. In addition, a comparative review of two widely used failure models, namely, total formulation and incremental formulation [2, 3], is carried out using Charpy impact test simulations where the failure parameters are prepared using the proposed method. It is found that the incremental formulation is excellent in predicting the experimentally observed behavior of notched Charpy impact test and un-notched Charpy impact test.

Introduction

Prediction of rupture behavior of products is a major objective for computer aided engineering simulation. Simulation results showing rupture behavior of products are very helpful in modifying the products. However it is challenging to prepare failure parameters to have good predictions of rupture behavior. The reasons are not only that the failure parameters depend on strain rate, stress triaxiality, and element size, but also that there are lots of failure models. In this paper, methods for preparing failure parameters available in SAMP-1 [1] are presented and a comparative review of two failure models known as total formulation [2, 3] and incremental formulation [2, 3] is also presented.

Experiment

Material and Specimen

In this study, a well-known ductile polymer material, polycarbonate, is used. The polycarbonate was also used in previous papers [4, 5] where mechanical properties of the polycarbonate have already been characterized using the SAMP-model.

In this study, ASTM D1822 Type-S specimen shown in Fig. 1 is used. The reason for use of the specimen comes from an idea that reproducibility of rupture displacement can easily be obtained in tensile test using this kind of specimens without gauge area [6].

High Speed Tensile Test

High-speed tensile test has been carried out using the ASTM D1822 Type-S specimen made of the polycarbonate. The considered tensile speed ranged from 8.3×10^{-6} to 5.0 m/sec. In this study, tensile test speeds up to 8.3×10^{-3} m/sec were conducted using a general purpose testing system (TEST-1) and remaining test speeds were conducted using a hydraulically-operated system (TEST-2). In each test stage, the number of specimens measured was at least 5 in TEST-1, and at least 3 in TEST-2.

Since the specimen does not have any gauge area, time history of tensile strain was not measured. Instead, time history data of tensile displacement between machine chucks and that of tensile load were measured so that tensile load – displacement relation can be obtained and can be used to check whether tensile test simulation predicts the experimental result. Rupture displacement of the specimen in each tensile speed was evaluated from the tensile load – displacement relation.

Fig. 2 shows an experimental result of rupture displacement – tensile speed relation obtained by the experiment. Rupture displacement shows decreasing trend with increasing tensile speed. Drastic decreasing around 3 m/sec tensile speed is also shown. All specimens ruptured in the vicinity of the center of the specimen.

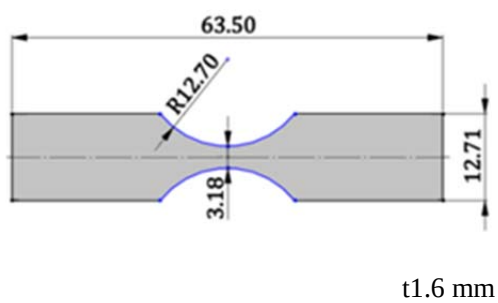

Fig. 1. ASTM D1822 type S specimen

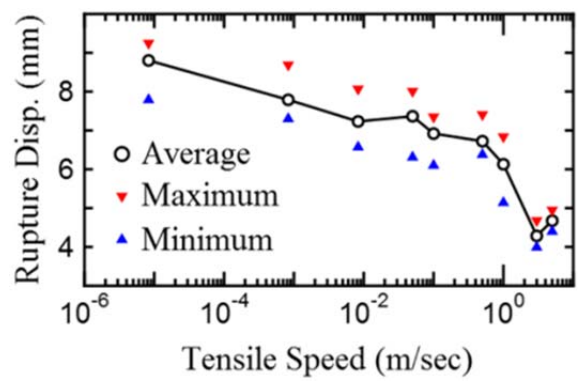

Fig. 2. Rupture displacement as a function tensile speed obtained in the experiments.

Failure Models in SAMP

The SAMP-model provides two failure formulations known as total formulation and incremental formulation via INCFAIL parameter [2, 3] as well as element size regularization [7]. The failure strain of the SAMP-model is "uniaxial tension/compression" equivalent plastic strain $\varepsilon_{\mathrm{eq,p}}^{\mathrm{u}}$ which is converted from equivalent plastic strain using Eq. 1,

$$\varepsilon_{\mathrm{eq,p}}^{\mathrm{u}} = \int_0^{\varepsilon_{\mathrm{eq,p}}} \sqrt{\frac{3}{2\left(1+\nu_{\mathrm{p}}\left(\varepsilon'_{\mathrm{eq,p}}\right)\right)}}\, d\varepsilon'_{\mathrm{eq,p}}\,, \qquad \text{Eq. 1}$$

where $\varepsilon_{\mathrm{eq,p}}$ is equivalent plastic strain, $\nu_{\mathrm{p}}(\varepsilon_{\mathrm{eq,p}})$ is plastic Poisson's ratio depending on equivalent plastic strain [1]. The "uniaxial tension/compression" equivalent plastic strain $\varepsilon_{\mathrm{eq,p}}^{\mathrm{u}}$ is obtained via history variable #2.

Total Formulation

This formulation is the conventional one as shown in Eq. 2,

$$\varepsilon_{\mathrm{failure}} \geq \varepsilon_{\mathrm{eq,p}}^{\mathrm{u}} = \sum \Delta\varepsilon_{\mathrm{eq,p}}^{\mathrm{u}}, \qquad \text{Eq. 2}$$

where $\varepsilon_{\mathrm{failure}}$ is failure strain, and $\Delta\varepsilon_{\mathrm{eq,p}}^{\mathrm{u}}$ is incremental "uniaxial tension/compression" equivalent plastic strain at each calculation step. In general, rupture behavior is affected by strain rate, stress triaxiality. In the SAMP-model, $\varepsilon_{\mathrm{failure}}$ is simply defined as shown in Eq. 3,

$$\varepsilon_{\mathrm{failure}} \equiv \varepsilon_{\mathrm{failure}}^{\mathrm{static}} F(\dot{\varepsilon}_{\mathrm{eq,p}}) G(\mu), \;\; \mu \equiv p/\sigma_{\mathrm{vm}} \qquad \text{Eq. 3}$$

where $\varepsilon_{\mathrm{failure}}^{\mathrm{static}}$ is failure strain at static state, p is pressure, σ_{vm} is von Mises equivalent stress, $F(\dot{\varepsilon}_{\mathrm{eq,p}})$ and $G(\mu)$ are scale factors as a function of strain rate $\dot{\varepsilon}_{\mathrm{eq,p}} = \Delta\varepsilon_{\mathrm{eq,p}}/\Delta t$, stress triaxiality μ, respectively. It is good to rewritten Eq. 2 as shown in Eq. 4 for comparison with the incremental formulation mentioned next,

$$\omega_{\mathrm{D}}' = \frac{1}{\varepsilon_{\mathrm{failure}}^{\mathrm{static}} F(\dot{\varepsilon}_{\mathrm{eq,p}}) G(\mu)} \sum \Delta\varepsilon_{\mathrm{eq,p}}^{\mathrm{u}} \,. \qquad \text{Eq. 4}$$

When the quantity ω_{D}' reaches 1, element erosion occurs.

Incremental Formulation

This formulation is regarded as a generalized Johnson-Cock damage model where cumulative damage is considered [8]. In the incremental formulation, incremental damage $\Delta\omega_{\mathrm{D}}$ in each calculation step is defined as shown in Eq. 5,

$$\Delta\omega_{\mathrm{D}} \equiv \frac{\Delta\varepsilon_{\mathrm{eq,p}}^{\mathrm{u}}}{\varepsilon_{\mathrm{failure}}} = \frac{\Delta\varepsilon_{\mathrm{eq,p}}^{\mathrm{u}}}{\varepsilon_{\mathrm{failure}}^{\mathrm{static}} F(\dot{\varepsilon}_{\mathrm{eq,p}}') G(\mu)} \,. \qquad \text{Eq. 5}$$

Accumulated damage ω_{D} is calculated as shown in Eq. 6,

$$\omega_{\mathrm{D}} = \sum \Delta\omega_{\mathrm{D}} = \sum \left\{ \frac{\Delta\varepsilon_{\mathrm{eq,p}}^{\mathrm{u}}}{\varepsilon_{\mathrm{failure}}^{\mathrm{static}} F(\dot{\varepsilon}_{\mathrm{eq,p}}') G(\mu)} \right\}. \qquad \text{Eq. 6}$$

When the accumulated damage ω_{D} reaches 1, element erosion occurs.

The scale factors $F(\dot{\varepsilon}_{\mathrm{eq,p}})$ and $G(\mu)$ in Eq. 6 works as weight factor for the incremental equivalent plastic strain. The major difference between two formulations is whether the weight

factors are included within the summation. When the scale factors are always unity, $F(\dot{\varepsilon}'_{\mathrm{eq,p}}) = 1.0$ and $G(\mu) = 1.0$, the two formulations are the same, $\omega_{\mathrm{D}} = \omega'_{\mathrm{D}}$.

Preparation of Parameters

Simulation Model

Fig. 3 shows one of FEM models used in this study to calibrate failure parameters as well as mechanical property such as stress – strain relation depending on strain rate [5]. The least element length of the specimen shown in Fig. 3 is 0.38 mm, and the elements locate at the center of the specimen. Four rigid plates are attached on the specimen as chucks of the testing system to elongate the specimen. The two plates in the left of the specimen are always fixed, while the other two plates are moved using prescribed motion with constant velocity. The history variable #2 is saved into ELOUT via OPTION1 of DATABASE_ELOUT offered by LS-DYNA Ver.971 R6 or later. In this study, LS-DYNA Ver.971 R6.1.1 is used.

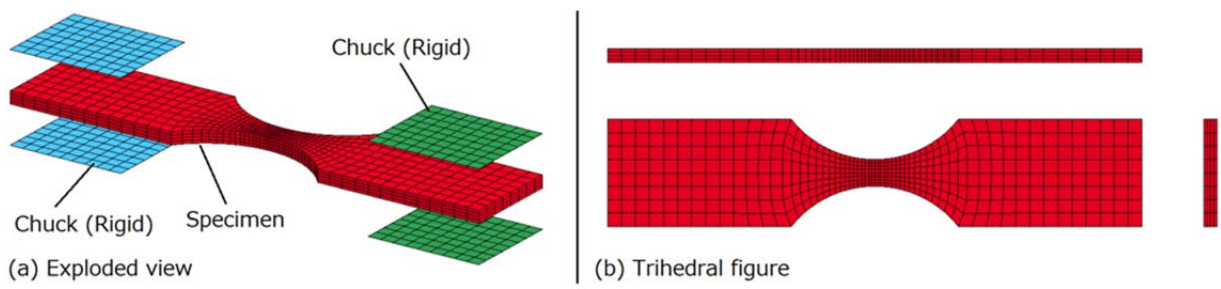

Fig. 3. One of FEM models used in this study. The least element length is 0.38 mm.
(a) Exploded view of the model, (b) Trihedral figure of the specimen.

Total Formulation of Failure

Evaluating the "uniaxial tension/compression" equivalent plastic strain $\varepsilon^{\mathrm{u}}_{\mathrm{eq,p}}$ is carried out in each simulation result predicting experimental result, such as tensile load – tensile displacement and necking behavior.

Fig. 4 shows the history variable #2, its time derivative and stress triaxiality as a function of tensile displacement at an element showing the largest value of the history variable #2 at failure time in the tensile test simulation at 1 m/sec in velocity. The stress triaxiality at failure time is almost -1/3 indicating that failure occurs in uniaxial tension state. A combination of failure strain 0.566 and strain rate 27 (1/sec) can be evaluated from the graph shown in Fig. 4. Tabulated data of failure strain as a function of strain rate can be obtained from the other simulation results at different tensile velocities. Fig. 5 shows the failure strain as a function of strain rate for the polycarbonate.

Fig. 6 shows scale factor $G(\mu)$ of failure strain depending on stress triaxiality μ used in this study. Since equi-biaxial tensile test was not carried out, scale factor at equi-biaxial stress state is tentatively set to 1.0. For uniaxial compression state, scale factor is set to 1.7 so that a compression specimen cannot be broken at 70% compression realized in experiments [4]. In this study, scale factor $G(\mu)$ from uniaxial tension state to uniaxial compression state is fitted using

Hancock-McKenzie failure criterion showing larger failure strain in compression state than tension state [9], and that for biaxial compression stress state is extrapolated. The Hancock-McKenzie failure criterion is given by Eq. 7,

$$G(\mu) = \exp[\alpha(\mu - \mu_{\mathrm{ut}})], \qquad \text{Eq. 7}$$

where α is a material constant, μ_{ut} is stress triaxiality factor at uniaxial tension state. In this study, the adjustable parameter α is set to 0.8. It should be noted that the failure parameters determined using the model shown in Fig. 3 is effective for models composing an element size 0.38 mm without element size regularization mentioned next.

Fig. 7 shows scale factor of failure strain for the element size regularization. The data is prepared using the similar method proposed by Effelsberg [7]. In this study, regularized results are obtained using the specimen models discretized by element sizes from 0.1 to 0.8 mm in the vicinity of the narrowest region.

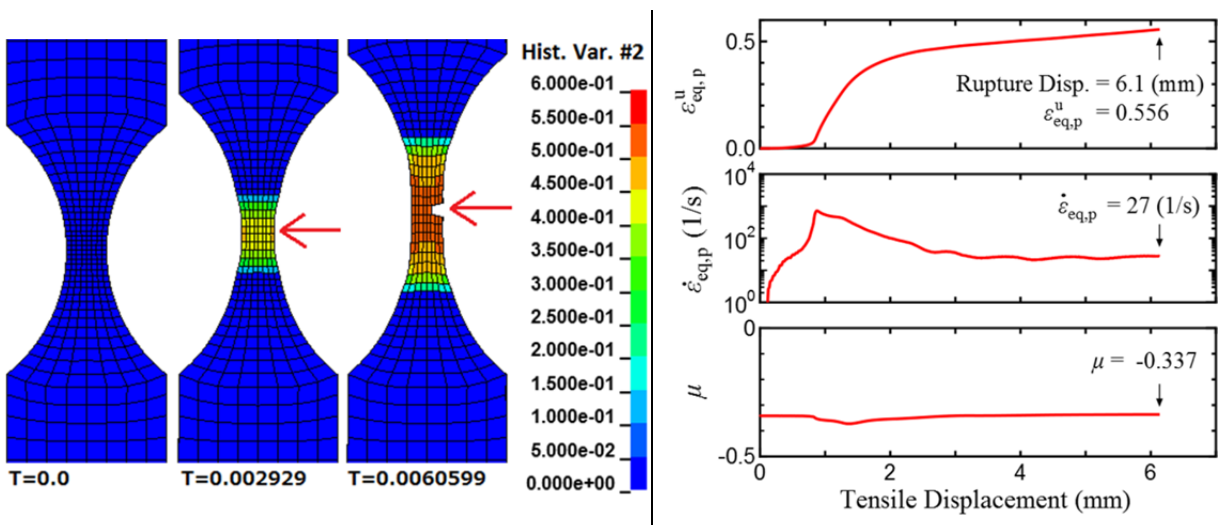

Fig. 4. (Left) Contour plot of the history variable #2 ($\varepsilon^{\mathrm{u}}_{\mathrm{eq,p}}$) on the specimen in the tensile test simulation at 1.0 m/sec velocity. Two arrows point to the highest distorted element at rupture displacement 6.1 mm. (Top right) Equivalent plastic strain history in the element pointed by the arrows in the left figure. (Middle right) Strain rate history in the element. (Bottom right) Stress triaxiality history in the element.

Incremental Formulation of Failure

The failure strain depending on strain rate for the total formulation has to totally be re-prepared for the incremental formulation. This is because strain rate shown in Fig. 4 drastically changes during tensile simulation due to necking behavior of the polycarbonate. Thus, Eq. 4 is not equal to Eq. 6.

Fig. 8 shows the comparison of failure strain as a function of strain rate between the total formulation and the incremental formulation for the polycarbonate studied. For strain rate less than 10 (1/s), failure strains for the incremental formulation are almost the same those for the total formulation. For strain rate more than 10 (1/s), failure strains for the incremental formulation have to be modified to have good prediction of rupture displacement.

In this study, scale factors for stress triaxiality and element size regularization prepared for the incremental formulation are the same those prepared for the total formulation.

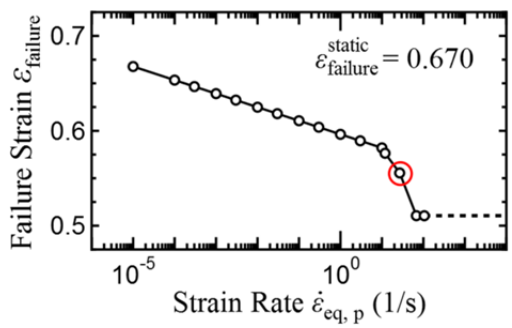

Fig. 5. Failure strain depending on strain rate determined for the total formulation. The point marked by red circle is the result (27, 0.566) from Fig. 4.

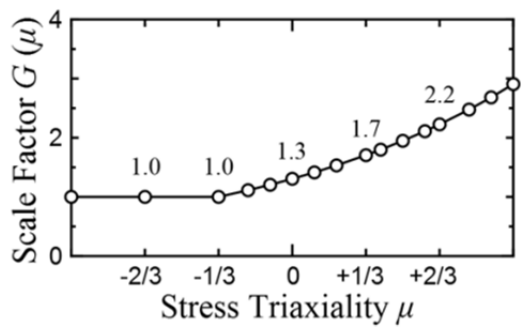

Fig. 6. Scale factor $G(\mu)$ as a function of stress triaxiality μ estimated for the polycarbonate used in this study.

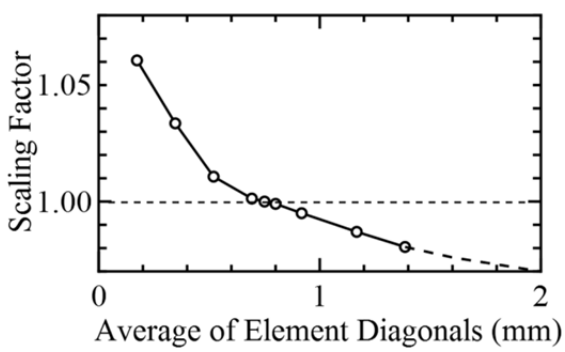

Fig. 7. Scale factors of the failure strain as a function of element size.

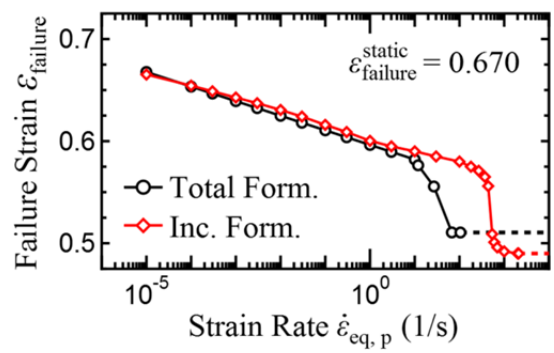

Fig. 8. Comparison of failure strain as a function of strain rate.

Analysis using Charpy Test

Notched Charpy test (JIS K7111-1/1eA) and un-notched Charpy test (JIS K7111-1/1eU) are chosen as validation tests for the failure formulations as well as the prepared parameters. Specimens in these tests are subjected to high strain rate loading, various stress state such as tension and compression stress states due to bending deformation of the specimen. Rate dependent parameters and stress state dependent parameters are necessary for accurate prediction of the tests.

Experimental Setups and Results

The geometry of specimen for the un-notched Charpy test was $4 \times 10 \times 80$ mm. The geometry of specimen for the notched Charpy test was the same, but its center was cut by

machining as shown in Fig. 9. Notched and un-notched Charpy tests have been conducted using 4J-hammer and 15J-hammer, respectively.

Fig. 10 (Left) shows experimental results for the notched Charpy test. One out of ten specimens was fully broken and nine specimens were subjected to hinge break. Averaged impact strength a_{cN} obtained from the nine specimens was 77±2 kJ/m^2.

Fig. 10 (Right) shows experimental results for the un-notched Charpy test. All specimens were not broken. Averaged impact strength a_{cN} was 320±7 kJ/m^2.

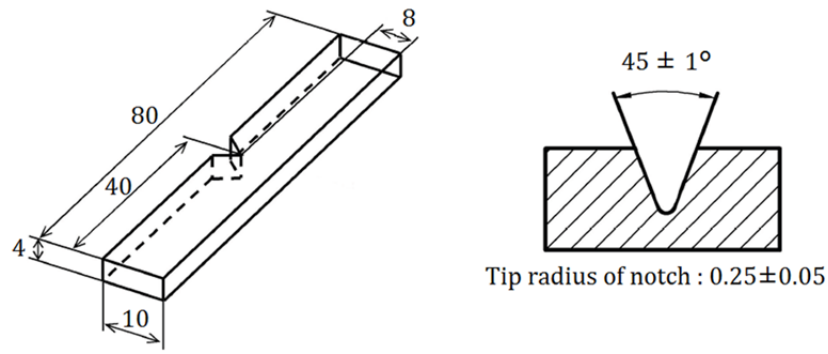

Fig. 9. Geometry of specimen for notched Charpy test (JIS K7111-1/1eA)

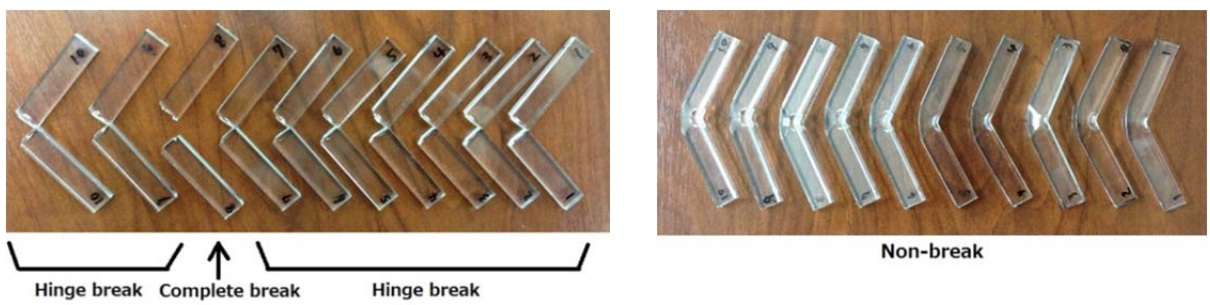

Fig. 10. Experimental results. (Left) Notched Charpy test, (Right) Un-notched Charpy test.

Simulation Setups

Fig. 11 and Fig. 12 show simulation models. The notch is discretized by fine mesh (0.15 mm) to have good prediction of rupture behavior as accurately as possible. Other area outside of the notch is discretized by relatively coarse mesh (0.32 mm) to reduce calculation cost. The element size regularization is necessary for the prediction of the good results. The element size for the un-notched Charpy specimen model is 0.4 mm.

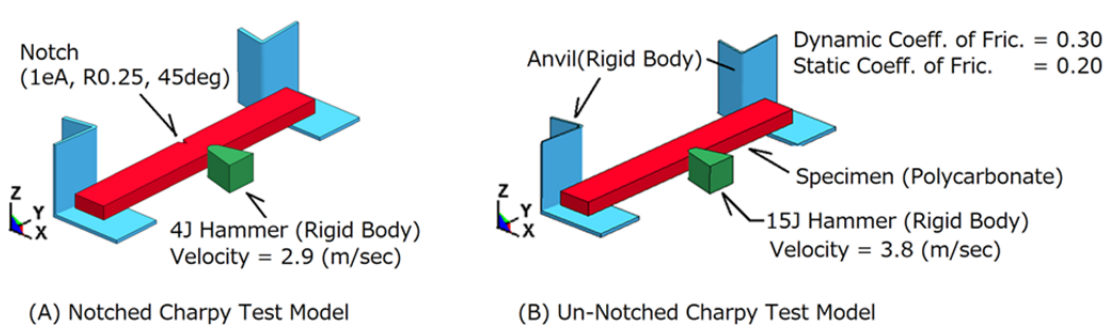

Fig. 11. Simulation models. (A) Notched Charpy test, (B) Un-notched Charpy test.

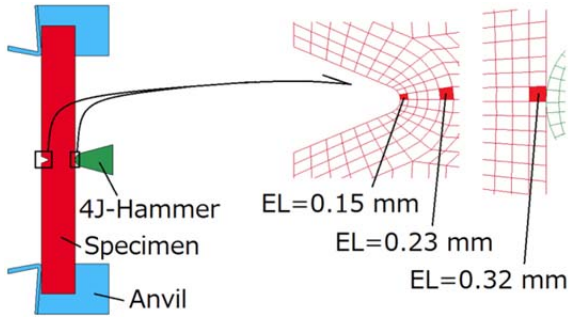

Fig. 12. Element discretization in the vicinity of the notched region.

Notched Charpy Test

Four simulation cases are considered as shown in Table 1. The stress triaxiality effect shown in Fig. 6 is considered for all the simulation cases.

Fig. 13 shows comparison of broken notches obtained from the four simulation cases. In the simulation cases (A) and (B), the specimens are subjected to hinge break. In the simulation cases (C) and (D), the specimens are subjected to partial break and the hammer is repulsed opposite direction in each case. Impact strength is evaluated using kinematic energy history of the hammer, and Impact strengths for the cases (A) and (B) are 85 and 95 kJ/m^2, respectively.

Table 1. Configuration table of four simulation cases studied.

	Total formulation	Inc. formulation
Failure strain with Rate dep.	(A)	(B)
Failure strain without Rate dep.	(C)	(D)

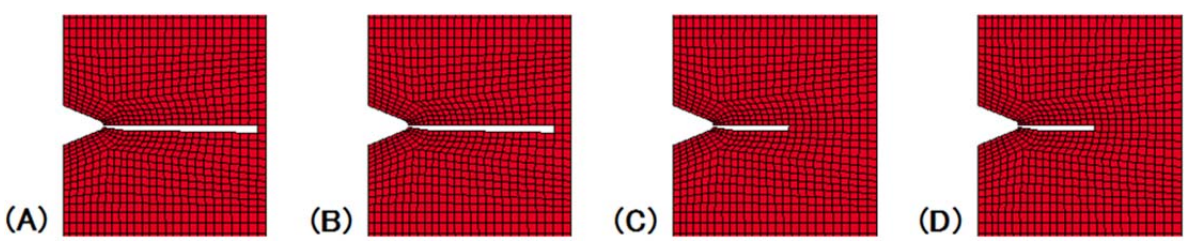

Fig. 13. Comparison of broken notches (max displacement factor is set to 0 for all axes.).

Un-Notched Charpy Test

Two simulation cases are considered, (A) and (B) shown in Table 1. Two simulation cases successfully predict deformation of specimen experimentally obtained as shown in Fig. 14 (Right). Impact strength for the both cases (A) and (B) is 275 kJ/m^2.

It is found that there is a significant difference of rupture behavior between simulation cases (A) and (B). The case (B) considering the incremental formulation shows no signs of rupture behavior, while the case (A) considering the total formulation shows unexpected element erosions around contact area of the specimen as shown in Fig. 14.

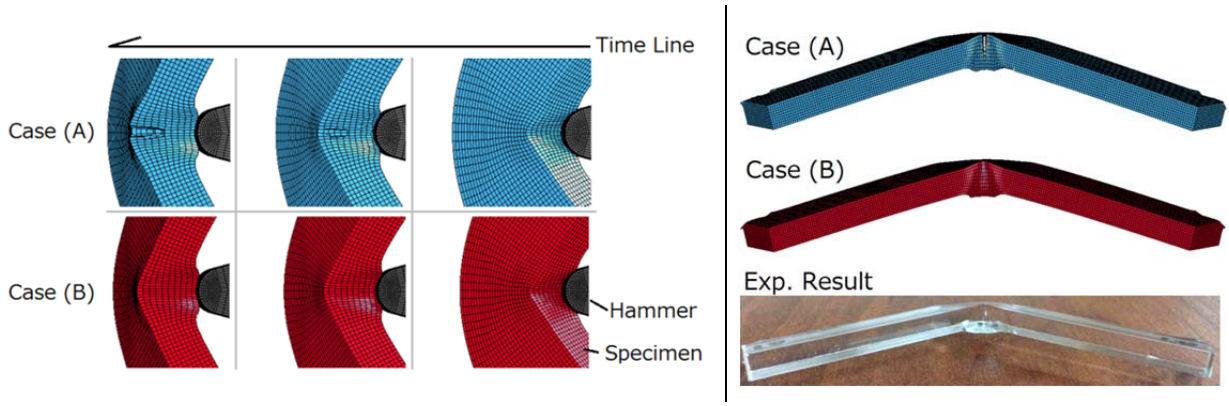

Fig. 14. (Left) A comparative view of simulation results in the vicinity of the center of the specimen. (Right) comparison of final state of specimens.

Discussion

Choice of Specimen

It is found that ASTM D1822 Type-S specimen is helpful in preparing the failure parameters. This is because rupture occurs in the vicinity of the center of the specimen in both experiment and simulation, making it easy to determine failure strain from simulation result. In contrast in a dog-bone type specimen, rupture occurs in gauge area, but its location randomly changes for every specimen, making it difficult to predict with simulation.

Un-Notched Charpy Test Simulation

Let us investigate the reason for the difference observed in the un-notched Charpy test simulation from the point of view of stress triaxiality. Fig. 15 shows time history of stress triaxiality contour plot for the simulation using the incremental formulation. In this time history, the elements of the specimen around contact area between the specimen and the hammer are initially subjected to compression stress state due to bending deformation of the specimen (ST=46, 52), and then the elements are subjected to tension stress state just before the specimen is released from anvil (ST=54). The unexpected element erosions occurs between the states ST=52 and ST=54 in the simulation using the total formulation.

The key to explain the reason is stress triaxiality. In the total formulation, contribution of the failure strain during compressive deformation is the same as that during tensile deformation. However in this study, for the incremental formulation with the prepared parameter, the contribution of the incremental damage $\Delta\omega_{\mathrm{D}}$ during compressive deformation is approximately half of that during tensile deformation due to "the weight factor $G(\mu)$" mentioned in Eq. 6, making it hard to realize element erosions in compression stress state.

It should be noted whether considering the incremental formulation is consistent with rupture behaviors experimentally observed. For ductile and thermo plastic materials, use of the incremental formulation would be appropriate. This is because rupture behavior usually occurs due to voids emerged in materials in tensile stress state, not in compression stress state.

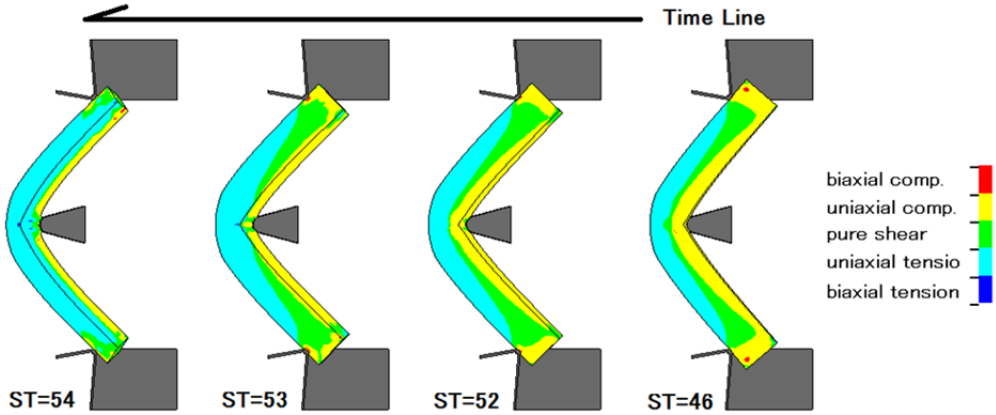

Fig. 15. Deformation history of the un-notched specimen predicted using the incremental formulation. Contour plot shows distribution of stress triaxiality.

Conclusion

The preparation method of failure parameters for the total formulation has been presented, and the difference of failure strain as a function strain rate between the total formulation and the incremental formulation has also been presented. Comparative reviews of the two formulations using notched and un-notched Charpy tests have been shown, and the incremental formulation of failure is found to have good prediction of failure behavior for the two Charpy tests as compared with the total formulation. The preparation method mentioned in the present study is very helpful in determining failure parameters for MAT_ADD_EROSION as well as the SAMP-model.

References

[1] S. Kolling, A. Haufe, M. Feucht and P. A. Du Bois, "SAMP-1: A Semi-Analytical Model for the Simulation of Polymers," 4th German LS-DYNA Users Forum Proceedings, A-II-27/57, 2005.

[2] P. A. Du Bois, M. Feucht, A. Haufe and S. Kolling, "A Generalized Damage and Failure Formulation for SAMP," LS-DYNA Anwenderforum, A-II-77/110, 2006.

[3] P. A. Du Bois, S. Kolling, M. Feucht and A. Haufe, "A Comparative review of damage and failure models and a tabulated genralization," 6th European LS-DYNA Users' Conf. Proceedings, pp. 75-84, 2007.

[4] K. Takekoshi and K. Niwa, "Validation and Material Modeling of Polymers by Employing MAT_SAMP-1," 12th International LS-DYNA Users Conference Proceedings, Constitutive Modeling05-C, 2012.

[5] K. Takekoshi and K. Niwa, "Study of Material Modeling of Polymers for Impact Analysis," Applied Mechanics and Materials, accepted.

[6] S. Okabe, "Impact Crack Forecast of Ductile Polymer Product by CAE (in Japanese)," JSME 23rd Computational Mechanics Division Conference Proceedings, p. 1306, 2010.

[7] J. Effelsberg, A. Haufe, M. Feucht, F. Neukamm, P. Du Bois, “On parameter identification for the GISSMO damage model,” 12th International LS-DYNA Users Conference Proceedings, Metal Forming(3), 2012.

[8] R. G. Johnson and H. W. Cook, "Fracture characteristics of three metals subjected to various strains, strain rates, temperatures and pressures.," Int. J. Eng. Fract. Mech., vol. 21, pp. 31-48, 1985.

[9] W. J. Hancock and C. A. Mckenzie, "On the mechanisms of ductile failure in high-strength steels subjected to multi-axial stress-states.," J. Mech. Phys. Solids, vol. 24, pp. 147-167, 1976.